On optimal feedforward and ILC

On Optimal Feedforward and ILC: The Role of Feedback for Optimal Performance and Inferential Control ⋆

Jurgen van Zundert * **Tom Oomen** *

* *Control Systems Technology, department of Mechanical Engineering, Eindhoven University of Technology, Eindhoven, The Netherlands (email: j.c.d.v.zundert@tue.nl)*

Abstract: The combination of feedback control with inverse model feedforward control or iterative learning control is known to yield high performance. The aim of this paper is to clarify the role of feedback in the design of feedforward controllers, with specific attention to the inferential situation. Recent developments in optimal feedforward control are combined with feedback control to jointly optimize a single performance criterion. Analysis and application show that the joint design addresses the specific control objectives. The combined design is essential in control, and in particular in inferential control.

Keywords: Inferential control, Optimal control, Feedforward control, Feedback control

1. INTRODUCTION

Many control applications involve both feedback and feedforward. Both are often tuned separately using specific approaches and based on different control goals, e.g., different norms. An example is iterative learning control (ILC) where the feedforward is designed as an add-on to feedback. This paper addresses the fundamental role of feedback in combination with feedforward and ILC, both for regular and inferential control.

The role of feedback is often assumed fixed in feedforward and ILC design, see e.g. Van der Meulen et al. (2008); Bristow et al. (2006), but also related approaches in Boeren et al. (2017). In fact, in Boeren et al. (2017) the performance of the feedforward controller depends on the feedback controller which is required to satisfy a certain assumption. Notable exceptions are Rogers et al. (2007), where it is advocated to use a 2D framework, and research on equivalent feedback (Goldsmith, 2002). In the present paper, the aim is to connect feedback and feedforward design.

Recent interest in inferential control, e.g. for mechatronics (Oomen et al., 2015; Ronde et al., 2012; Voorhoeve et al., 2016), has led to a new interest in controller structures. Inferential control imposes an additional constraint on how to design feedforward and feedback that jointly optimize a single performance criterion, which is not immediate in such situations as pointed out in Bolder and Oomen (2016). However, at present limited guidelines are available how to actually design the controller. In the present paper, the joint design of feedback with feedforward/ILC in a two degrees-of-freedom inferential control architecture is investigated.

Although there have been important developments in ILC and feedforward design frameworks, the role of feedback is often not explicitly addressed. The aim of this paper is to clarify the role of feedback in the design of feedforward controllers, with specific attention to both the regular and the inferential situation. The method follows from recent developments of norm-optimal ILC and feedforward algorithms in Van Zundert et al. (2016). The algorithms are used to show the role of feedback and feedforward in achieving optimal performance, thereby confirming the claim related to the assumption $SH = 1$ in Boeren et al. (2017). It is also shown that this gives a direct solution to the inferential control problem, providing a solution that falls within the controller structures outlined in the framework of Oomen et al. (2015). As such, the present paper extends Van Zundert et al. (2016) in these two aspects.

The outline of the paper is as follows. In section 2, the regular and inferential control problems are formulated. The inferential control application of a wafer stage is presented in section 3. In section 4, the control design for the regular case $z = y$ is presented. In section 5, the control design for the inferential case $z \neq y$ is presented. Application to iterative learning control (ILC) is presented in section 6. Section 7 contains conclusions.

2. PROBLEM FORMULATION

In this section the control objective is formulated. The formulation is split into two parts: the standard control problem with $z = y$ and the inferential control problem with $z \neq y$.

⋆ This research is supported by the Dutch Technology Foundation STW, carried out as part of the Robust Cyber-Physical Systems (RCPS) project (no. 12694); and Innovational Research Incentives Scheme under the VENI grant "Precision Motion: Beyond the Nanometer" (no. 13073) awarded by NWO (The Netherlands Organization for Scientific Research).

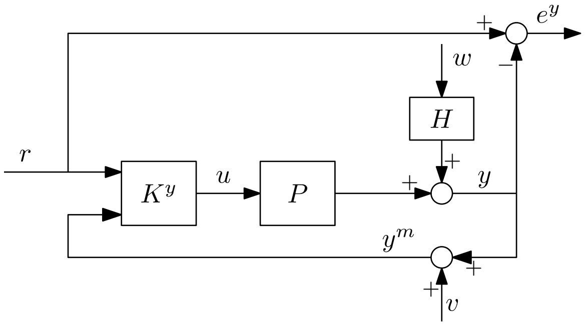

Fig. 1. Two degrees-of-freedom tracking control architecture for $z = y$ with inputs reference trajectory r and measurement y^m. The control objective is tracking r with y.

2.1 Control for $z = y$

Consider the system

$$
\begin{aligned}
x_{k+1} &= Ax_k + Bu_k + Gw_k, \\
y_k &= C^y x_k + H^y w_k, \\
y_k^m &= y_k + v_k,
\end{aligned} \tag{1}
$$

with state $x_k \in \mathbb{R}^{n_x}$, input $u_k \in \mathbb{R}^{n_i}$, output $y_k \in \mathbb{R}^{n_o}$, output measurement $y_k^m \in \mathbb{R}^{n_o}$, process noise $w_k \in \mathbb{R}^{n_x}$, and measurement noise $v_k \in \mathbb{R}^{n_o}$, where

$$
w \sim \mathcal{N}(0, \sigma_w^2 I_{n_x}), \qquad v \sim \mathcal{N}(0, \sigma_v^2 I_{n_o}),
$$

with variances $\sigma_w^2, \sigma_v^2 \in \mathbb{R}^+$.

In order to have y track a pre-specified reference trajectory r, the two degrees-of-freedom control architecture in Fig. 1 is considered where

$$
P \overset{s}{=} \left[\begin{array}{c|c} A & B \\ \hline C^y & 0 \end{array}\right], \qquad H \overset{s}{=} \left[\begin{array}{c|c} A & G \\ \hline C^y & H^y \end{array}\right].
$$

The control objective is the design of controller K^y to minimize $e^y = r - y$, with measurement y^m of y available.

Remark 1. For notation convenience, it is assumed that system (1) is time-invariant and without direct feedthrough from u. However, all results can readily be extended to the more general case of time-varying systems and systems with direct feedthrough.

2.2 Control for $z \neq y$

In inferential control there are no means to directly measure the point of interest z. Instead, only measurements y of other locations are available. This control challenge may arise from undesired flexibility in the system, as in the printer application of Fig. 2(a), or from the inability to measure at the desired location, as in the wafer stage application of Fig. 2(b).

For an inferential setting, $z \neq y$, (1) is extended with

$$
z_k = C^z x_k.
$$

The extended control architecture is shown in Fig. 3, where

$$
P^z \overset{s}{=} \left[\begin{array}{c|c} A & B \\ \hline C^z & 0 \end{array}\right], \qquad H^z \overset{s}{=} \left[\begin{array}{c|c} A & G \\ \hline C^z & 0 \end{array}\right].
$$

The control objective is the design of K^z to minimize $e^z = r - z$, with only measurements y^m of y available.

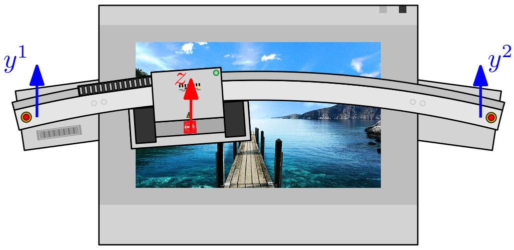

(a) High accelerations of the print heads induce deformations of the gantry causing mismatches between measured positions y_1, y_2 and the actual print head position z.

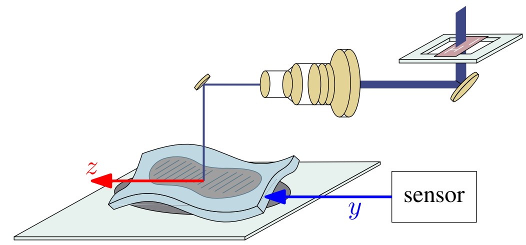

(b) In wafer scanner systems, an optical column directs light to the light sensitive layers of the wafer. The optical column hampers position measurement of the exposed performance location z. Instead, the edge of the wafer stage y is measured.

Fig. 2. Examples of inferential control problems. Performance location z cannot be measured and only measurements y are available.

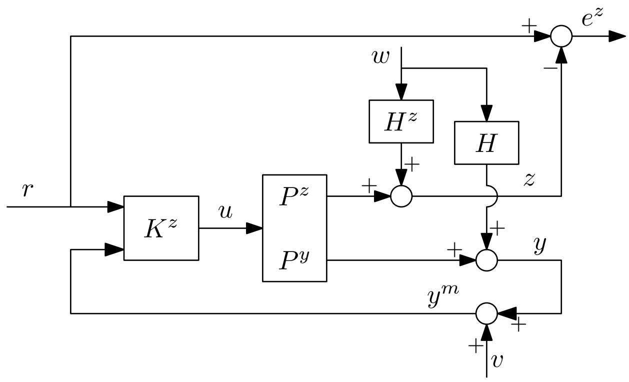

Fig. 3. Two degrees-of-freedom tracking control architecture for inferential control where performance variable and measurement are different: $z \neq y$. The control objective is tracking r with z.

3. WAFER STAGE APPLICATION

Wafer stages are key components in wafer scanners used for the production of integrated circuits. The stages accurately position the wafer during exposure.

The considered system is a simplified version of the wafer stage in Fig. 2(b) which is assumed to be a rigid body, see Fig. 4. The wafer stage is actuated by force F and can translate in q_1, q_2 and rotate in ϕ. The point of interest z cannot be measured due to the optical column used for exposure. Instead, the edge of the stage y is measured with a sensor that is located on the fixed world yielding measurement y^m. Note that if there are no rotations, i.e., $\phi = 0$, then $z = y$, otherwise $z \neq y$.

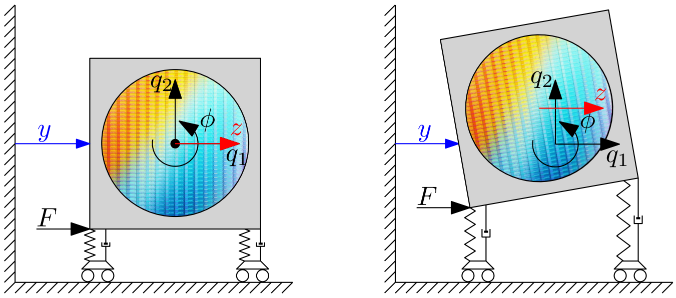

(a) Position y corresponds with point of interest z: $z = y$.

(b) Rotations of the stage introduce a mismatch in position: $z \neq y$.

Fig. 4. Top view of wafer stage model revealing the inferential control challenge as $z \neq y$ for $\phi \neq 0$.

Table 1. Parameter values of the wafer stage model.

parameter	symbol	value	unit
mass	m	8	kg
inertia	I	0.0133	kgm^2
spring constant	k	10^4	N/m
damping constant	d	100	Ns/m
length	l	0.1	m

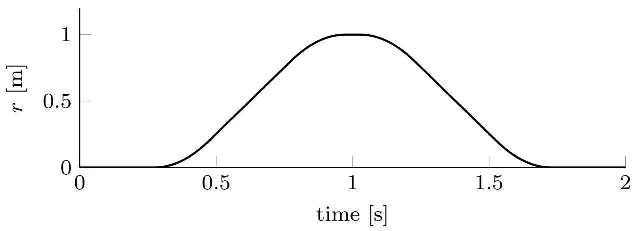

Fig. 5. Reference trajectory r of length $N = 2001$ samples.

A linearized model of the system in Fig. 4 is considered, see also (Van Zundert et al., 2016, sec. 3.4). The *continuous-time* state-space realization of the linearized system dynamics with input F, state $q = \begin{bmatrix} q_1 & \dot{q}_1 & \phi & \dot{\phi} \end{bmatrix}^\top$, and output y is

$$\left[\begin{array}{c|c} A_c & B_c \\ \hline C_c^y & 0 \end{array}\right] = \left[\begin{array}{cccc|c} 0 & 1 & 0 & 0 & 0 \\ 0 & 0 & 0 & 0 & \frac{1}{m} \\ 0 & 0 & 0 & 1 & 0 \\ 0 & 0 & -\frac{1}{2}\frac{kl^2}{I} & -\frac{1}{2}\frac{dl^2}{I} & \frac{1}{2}\frac{l}{I} \\ \hline 1 & 0 & 0 & 0 & 0 \end{array}\right].$$

Assuming zero-order-hold on the input, the discretized system has a state-space realization

$$P^y \stackrel{s}{=} \left[\begin{array}{c|c} A & B \\ \hline C^y & 0 \end{array}\right] = \left[\begin{array}{c|c} e^{A_c h} & A_c^{-1}(A - I)B_c \\ \hline C_c^y & 0 \end{array}\right],$$

with sample time $h = 0.001$ s. The parameters are listed in Table 1. Furthermore, $G = I_4$ and $H^y = 0_{1\times 4}$ in (1), with noise variances $\sigma_w^2 = 10^{-6}$, $\sigma_v^2 = 10^{-10}$.

The reference trajectory r consists of a fourth-order forward and backward motion and is provided in Fig. 5.

4. APPLICATION TO $z = y$

In this section, it is assumed that performance variable z can be measured, i.e., $z = y$ ($C^z = C^y$).

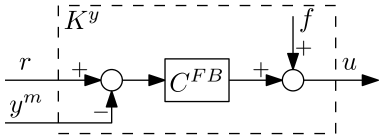

Fig. 6. Standard feedback/feedforward control.

4.1 Analysis

A common control architecture consisting of feedback controller C^{FB} and feedforward f is shown in Fig. 6. Implementation of this controller in the diagram of Fig. 1 yields

$$e^y = S(r - Pf) - SHw + SPC^{FB}v, \tag{2}$$

with sensitivity $S = \left(I + PC^{FB}\right)^{-1}$.

The first term in (2) is completely deterministic and can be influenced by both feedback and feedforward. Note that the term cannot be fully eliminated using feedback C^{FB} since $S = 0$ is not feasible due to Bode's sensitivity integral (Seron et al., 1997). In contrast, the term can be fully eliminated by feedforward $f = P^{-1}r$.

The second and third term in (2) are stochastic and can therefore not be completely eliminated. Both terms can only be influenced by feedback. Assuming that the first term in (2) is eliminated by feedforward $f = P^{-1}r$ and that there is no measurement noise, i.e., $v = 0$, then $e^y = -SHw$. This error has minimal variance if it is white. This imposes the condition

$$SH = 1, \tag{3}$$

corresponding to Assumption 2.1 in Boeren et al. (2017).

4.2 Optimal control

The optimal control law is derived from norm-optimal ILC.

ILC Given data e_j, f_j of current trial j, norm-optimal ILC determines feedforward f_{j+1} for next trial $j+1$ that minimizes

$$\|e_{j+1}\|_{w_e}^2 + \|f_{j+1}\|_{w_f}^2 + \|f_{j+1} - f_j\|_{w_{\Delta f}}^2, \tag{4}$$

with $w_e, w_f, w_{\Delta f} \in \mathbb{R}^+$, where $\|(\cdot)\|_w^2 = (\cdot)^\top w(\cdot)$. A common solution method for norm-optimal ILC is lifted ILC which is based on describing input-output relations in lifted/supervector notation (Moore, 1993). In Van Zundert et al. (2016) it is shown that the computation time of the lifted solution method grows as $\mathcal{O}(N^3)$, with N the task length. Moreover, an alternative resource-efficient solution method based on Riccati equations is presented. The method yields exactly the same results, but the computation time grows as $\mathcal{O}(N)$. In the remainder of this section and section 5, the focus is on feedforward control. See section 6 for ILC.

Feedforward Feedforward can be seen as a special case of ILC in which only one trial is performed, i.e., with $w_{\Delta f} = 0$. Consequently, (4) reduces to the LQ criterion

$$\sum_{k=0}^{N-1} (e_k^y)^\top Q(e_k^y) + (u_k)^\top R(u_k). \tag{5}$$

The weights are selected as $Q = w_e = 10^{10}$, $R = w_f = 10^{-10}$ to minimize e^y with minimal restriction on u. The optimal resource-efficient solution is given by Lemma 2.

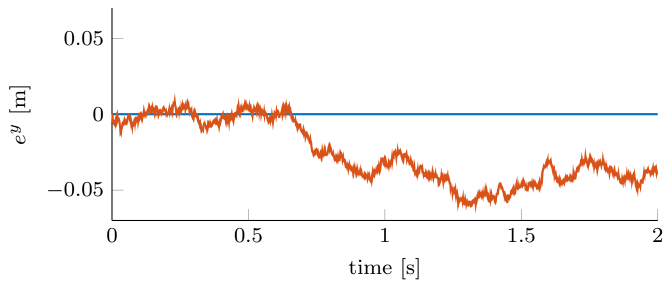

Fig. 7. Perfect tracking for (8) on the system *without* noise (——) deteriorates under the presence of noise (——).

Lemma 2. (Optimal feedforward). Input u for (1) with $w, v = 0$ that minimizes (5) is given by

$$u_k^* = -K_k x_k + L_k^g g_{k+1}, \tag{6}$$

with

$$\begin{aligned} P_k &= -A^\top P_{k+1} B (R + B^\top P_{k+1} B)^{-1} B^\top P_{k+1} A \\ &\quad + A^\top P_{k+1} A + (C^y)^\top Q (C^y), \qquad P_N = 0_{n_x \times n_x}, \\ g_k &= \left(-A^\top P_{k+1} \left(I + B R^{-1} B^\top P_{k+1}\right)^{-1} B R^{-1} B^\top \right. \\ &\quad \left. + A^\top \right) g_{k+1} + (C^y)^\top Q r_k, \qquad q_N = 0_{n_x \times 1}, \\ K_k &= \left(R + B^\top P_{k+1} B\right)^{-1} B^\top P_{k+1} A, \\ L_k^g &= \left(R + B^\top P_{k+1} B\right)^{-1} B^\top. \end{aligned} \tag{7}$$

Proof. Follows from setting $w_{\Delta f} = 0$ and $D = 0$ in Theorem 6 of Van Zundert et al. (2016).

Next, optimal input (6) is used for design of K^y in Fig. 1.

4.3 Feedforward approach

For the case without noise, i.e., $v, w = 0$, (2) reduces to

$$e^y = S(r - Pf)$$

which is completely deterministic. Perfect tracking can be obtained through feedforward only by selecting, see also Lemma 2,

$$u_k = f_k^*, \tag{8}$$

with

$$f_k^* = -K_k x_k^* + L_k^g g_{k+1}. \tag{9}$$

Since (1) is completely deterministic for $v, w = 0$, optimal state x^* can be calculated a priori as

$$x_{k+1}^* = (A - BK_k) x_k^* + B L_k^g g_{k+1}. \tag{10}$$

Note that this approach is also followed in Van Zundert et al. (2016) for feedforward design.

Fig. 7 shows excellent tracking for (8) on the wafer stage system of section 3 *without* noise ($v, w = 0$). Note that $e^y = 0$ if $\frac{Q}{R} \to \infty$ in (5), whereas (7) requires $R > 0$ to avoid singularity. The results confirm the analysis in section 4.1 that the first term in (2) can be fully eliminated by feedforward.

Fig. 7 also shows the results for (8) on the true system *with* noise ($v, w \neq 0$). Clearly, the high performance is deteriorated by the noise. Note that since (8) consists of feedforward only, $C^{FB} = 0$, $S = 1$ in (2) such that

$$e^y = (r - Pf) - Hw = -Hw, \tag{11}$$

since (8) eliminates the first term as shown without noise.

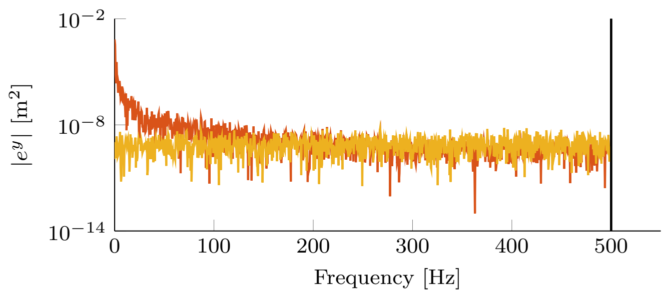

Fig. 8. The spectrum of e^y for (12) (——) is flat confirming optimality, whereas for (8) (——) it is colored confirming non-optimality.

4.4 Combined feedforward and feedback

The previous section shows that feedforward control can eliminate all reference induced errors, but cannot compensate for noise induced errors. In contrast, feedback control can compensate for noise induced errors, see also section 4.1. A key observation is that (6) includes state feedback on state x, but that this is not exploited in (8) by replacing x with x^* in (10) assuming a noise free system. In the proposed approach, feedback in (6) is exploited to suppress the noise induced errors.

Combined feedforward and optimal state feedback Optimal control law (6) can be rewritten as

$$u_k = -K_k \Delta x_k + f_k^*, \tag{12}$$

with f_k^* in (9) and

$$\Delta x_k = x_k - x_k^*$$

the deviation of the true state from the optimal state (10). Control input (12) consists of feedforward and state feedback, and assumes that x is available. Since (12) uses state x rather than y^m for feedback, v is not fed back in (2) such that

$$e^y = S(r - Pf) - SHw.$$

Feedforward f^* eliminates all reference induced errors, i.e., the first term, as shown by section 4.3. Since the feedback control is optimal it satisfies (3), and yields minimal variance on e^y by creating $SH = 1$.

The spectrum of e^y for application on the wafer stage system of section 3 is shown in Fig. 8. The figure shows that the feedback control in (12) yields a flat spectrum of e^y, confirming whiteness and thus optimality. Fig. 8 also shows that the spectrum of e^y is not flat for (8), indicating non-optimality of the feedforward only approach.

Combined feedforward and output feedback Control (12) assumes that true state x is available, which is generally not the case. Therefore, x is replaced by an estimate $\hat{x}$ that is obtained through a Kalman filter on the measurable output y^m as given by Lemma 3.

Lemma 3. (Kalman filter). State x and output y of system (1) can be estimated from y^m by

$$\begin{aligned} \hat{x}_{k+1} &= A\hat{x}_k + Bu_k + L_k(y_k^m - \hat{y}_k), \\ \hat{y}_k &= C^y \hat{x}_k, \end{aligned} \tag{13}$$

with gain matrix

$$L_k = (X_k (C^y)^\top + \bar{N})(C^y X_k (C^y)^\top + \bar{R})^{-1},$$

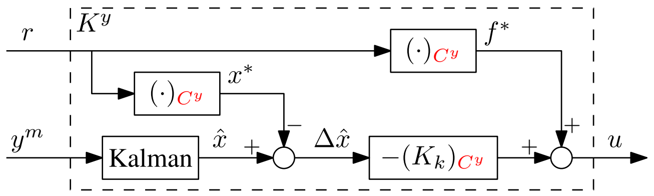

Fig. 9. Optimal feedforward control and observer based output feedback control implementation. The feedback control is based on state estimate $\Delta\hat{x}$ obtained through a Kalman filter from measurement y^m.

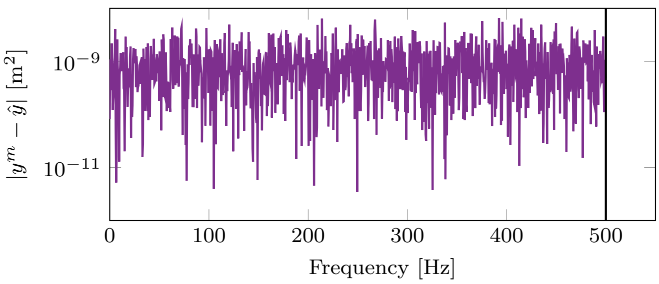

Fig. 10. Innovation $y^m - \hat{y}$ of the Kalman filter (13) under control (14) has a flat spectrum confirming optimality.

where X is the solution of the discrete-time dynamic Riccati equation

$$X_{k+1} = -AX_k(C^y)^\top(C^yX_k(C^y)^\top + R_n)^{-1}C^yX_kA^\top + AX_kA^\top + Q_n, \qquad X_0 = 0_{n_x \times n_x},$$

and

$$\bar{R} = R_n + H^yN_n + N_n^\top(H^y)^\top + H^yQ_n(H^y)^\top,$$
$$\bar{N} = G(Q_n(H^y)^\top + N_n),$$
$$Q_n = \sigma_w^2 I_{n_x}, \quad R_n = \sigma_v^2 I_{n_o}, \quad N_n = 0_{n_x \times n_o}.$$

Proof. See, for example, Anderson and Moore (1989).

Replacing Δx in (12) by $\Delta\hat{x}_k = \hat{x}_k - x_k^*$ yields

$$u_k = -K_k\Delta\hat{x}_k + f_k^*. \tag{14}$$

This combination of feedforward control and observer based output feedback control is similar to linear quadratic Gaussian (LQG) control, with the key difference that here an explicit split in feedback and feedforward is made. The complete control structure is shown in Fig. 9.

Controller (14) consists of feedforward and feedback. Feedforward f^* eliminates all reference induced errors, as shown in section 4.3. Feedback control $-K_k\Delta\hat{x}_k$ yields minimal variance on e^y if $v = 0$ since then $\hat{x} = x$ and (11) is recovered. Similar as for the traditional feedback controller, optimality of Kalman filter (13) is achieved when the input, i.e., innovation $y^m - \hat{y}$, is white.

Fig. 10 and Fig. 11 show the results for (14) on the wafer stage application of section 3. Fig. 10 shows that the innovation indeed has a flat spectrum, confirming optimality of the Kalman filter. Fig. 11 shows that the combined feedforward/feedback approach (14) outperforms the feedforward only approach (8) since it compensates for disturbances through feedback.

In summary: controller K^y with optimal feedforward requires feedback control to whiten trial-varying disturbances and a Kalman filter to whiten measurement noise.

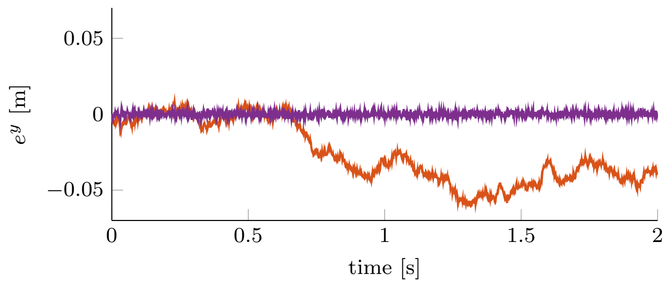

Fig. 11. The combined feedback and feedforward approach (14) (——) achieves high performance, outperforming the feedforward only approach (8) (——).

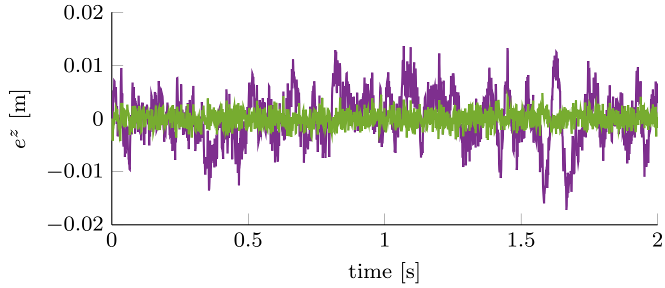

Fig. 12. The performance in terms of e^z for (14) is poor when based on C^y (——), but good when based on C^z (——).

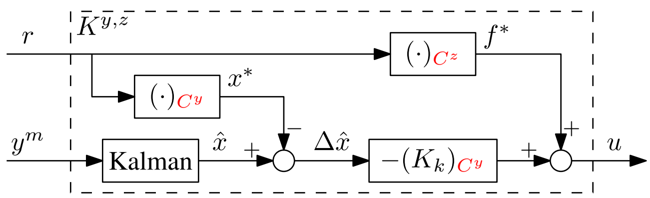

Fig. 13. Controller implementation in an inferential setting $z \neq y$, where the feedforward is optimized for z and the feedback for y.

5. APPLICATION TO $z \neq y$

In this section, the inferential control problem is considered where performance variable z differs from output y, i.e., $z \neq y$. Here,

$$C^z = \begin{bmatrix} 1 & 0 & \frac{2}{5}l & 0 \end{bmatrix}.$$

Fig. 11 shows that (14) yields excellent performance in terms of e^y. However, Fig. 12 shows that the performance in terms of $e^z = r - z$ is poor. The results indicate the importance of proper control architecture design.

The performance is often improved by design of feedforward f^* for z such that it minimizes e^z, see Fig. 13. However, the design in Fig. 13 creates a hazardous situation since the feedforward regulates for z, while the feedback regulates for y. Indeed, if the feedforward is optimal and yields $e^z = 0$, then it is counteracted by feedback control since generally $e^y \neq 0$ if $e^z = 0$ and the high performance of feedforward is deteriorated. Instead, feedback and feedforward control should have a common objective.

Both the feedback and feedforward control should be designed for z as shown in Fig. 14. The combined feedback and feedforward design proposed in section 4 guarantees a

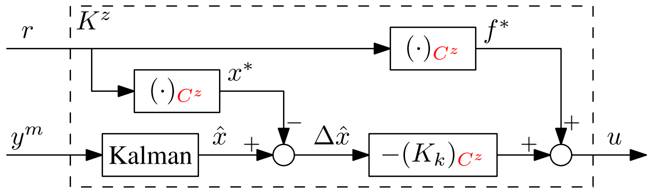

Fig. 14. Controller implementation in an inferential setting $z \neq y$, where both feedback and feedforward are explicitly designed for z.

common objective for feedback and feedforward. For $z \neq y$, criterion (5) changes to

$$\sum_{k=0}^{N-1} (e_k^z)^\top Q(e_k^z) + (u_k)^\top R(u_k). \tag{15}$$

The optimal solution that minimizes (15) directly follows from replacing C^y in Lemma 2 with C^z. Note that this indeed affects both feedback K and feedforward f^* in (14), see also Fig. 14. Importantly, Lemma 3 remains unchanged since it uses measurement y^m and should therefore be based on C^y.

Fig. 12 shows the results for the combined control approach based on criterion (15). As a result of the common objective in feedback and feedforward, the explicit design for z outperforms the design for y in terms of e^z.

In summary: a two degrees-of-freedom control architecture is crucial in inferential control, in conjunction with the whitening of the feedback and Kalman filter of section 4.

6. ITERATIVE LEARNING CONTROL

In this section, the combined design in an ILC setting is analyzed. Whereas inverse model feedforward requires high quality models, ILC can compensate for model mismatches.

The inferential case $z \neq y$ is of particular interest due to the feedback mechanism over trials present in the feedforward update. As pointed out in Bolder and Oomen (2016), the feedback action on y is iteratively compensated by the feedforward update, resulting in counteracting feedback and feedforward action. Similar as for feedforward, both feedback and ILC should be designed on z. The ILC performance objective in terms of $e^z_{k,j+1}$ reads

$$\sum_{k=0}^{N-1} (e^z_{k,j+1})^\top w_e(e^z_{k,j+1}) + (u_{k,j+1})^\top w_u(u_{k,j+1}) \\ + (u_{k,j+1} - u_{k,j})^\top w_{\Delta u}(u_{k,j+1} - u_{k,j}),$$

where j indicates the current trial and $j+1$ the next trial. The solution is a straightforward extension of the results for the feedforward case, see section 4 and section 5.

7. CONCLUSION

For the regular case $z = y$, the combined feedback and feedforward controller K^y should be designed such that trial-varying disturbances are whitened by feedback.

For the inferential case $z \neq y$, a two degrees-of-freedom control architecture is crucial, in conjunction with the whitening of feedback. Norm-optimal ILC automatically provides this solution, but care should be taken, see also (Doyle, 1978).

In ILC, the rationale is that the system model is approximate, which is compensated through iterations, motivating that alternative frameworks may be essential, see also Doyle (1978). Still, the results are of conceptual interest: 1) $SH = 1$ is a sensible assumption/control goal for disturbance rejection, and 2) inferential control needs additional attention on controller structures.

REFERENCES

Anderson, B.D. and Moore, J.B. (1989). *Optimal Control: Linear Quadratic Methods*, volume 1. Prentice Hall International, Inc., Englewood Cliffs, New Jersey.

Boeren, F., Bruijnen, D., and Oomen, T. (2017). Enhancing feedforward controller tuning via instrumental variables: with application to nanopositioning. *International Journal of Control*, 90(4), 746–764.

Bolder, J. and Oomen, T. (2016). Inferential Iterative Learning Control: A 2D-system approach. *Automatica*, 71, 247–253.

Bristow, D., Tharayil, M., and Alleyne, A. (2006). A Survey of Iterative Learning Control. *Control Systems Magazine*, 26(3), 96–114.

Doyle, J.C. (1978). Guaranteed Margins for LQG Regulators. *Transactions on Automatic Control*, 23(4), 756–757.

Goldsmith, P.B. (2002). On the equivalence of causal LTI iterative learning control and feedback control. *Automatica*, 38(4), 703–708.

van der Meulen, S.H., Tousain, R.L., and Bosgra, O.H. (2008). Fixed Structure Feedforward Controller Design Exploiting Iterative Trials: Application to a Wafer Stage and a Desktop Printer. *Journal of Dynamic Systems, Measurement, and Control*, 130(5), 051006:1–16.

Moore, K.L. (1993). *Iterative Learning Control for Deterministic Systems*. Springer-Verlag.

Oomen, T., Grassens, E., and Hendriks, F. (2015). Inferential Motion Control: Identification and Robust Control Framework for Positioning an Unmeasurable Point of Interest. *Transactions on Control Systems Technology*, 23(4), 1602–1610.

Rogers, E., Galkowski, K., and Owens, D.H. (2007). *Control Systems Theory and Applications for Linear Repetitive Processes*, volume 349. Springer.

Ronde, M., van de Molengraft, R., and Steinbuch, M. (2012). Model-based feedforward for inferential motion systems, with application to a prototype lightweight motion system. In *American Control Conference*, 5324–5329.

Seron, M.M., Braslavsky, J.H., and Goodwin, G.C. (1997). *Fundamental Limitations in Filtering and Control*. Springer-Verlag.

Voorhoeve, R., Dirkx, N., Melief, T., Aangenent, W., and Oomen, T. (2016). Estimating structural deformations for inferential control: a disturbance observer approach. In *Proceedings of the 7th IFAC Symposium on Mechatronic Systems*, 642–648. Loughborough, UK.

van Zundert, J., Bolder, J., Koekebakker, S., and Oomen, T. (2016). Resource-efficient ILC for LTI/LTV systems through LQ tracking and stable inversion: Enabling large feedforward tasks on a position-dependent printer. *Mechatronics*, 38, 76–90.